Thermally stimulated electron delocalization and luminescence quenching of Ce impurities in $GdAlO_3$

E. van der Kolk, P. Dorenbos, J. T. M. de Haas, and C. W. E. van Eijk
Faculty of Applied Sciences, Delft University of Technology, Mekelweg 15, 2629 JB Delft, The Netherlands
(Received 28 July 2004; published 25 January 2005)

A combined photoconductivity and luminescence quenching study, both temperature and spectrally resolved, has revealed the role played by electron delocalization in luminescence quenching of Ce^{3+} impurities in the wide band-gap inorganic insulator $GdAlO_3$. The anticorrelation found between the temperature behavior of photocurrent and luminescence intensity strongly suggests that luminescence quenching and photoconduction are intimately related by the same process, i.e., thermal stimulated ionization of optically excited Ce^{3+} centers: $Ce^{3+} \rightarrow Ce^{4+}$ + electron. Quantitative modeling of experimental data using rate equations, however, reveals a 0.05-eV smaller activation energy for luminescence quenching than for photocurrent generation which indicates that quenching predominantly proceeds via the formation of a Ce bound exciton at the originally excited Ce ion. A second quenching process, dominant below 230 K, seems mediated by energy transfer from Ce^{3+} via the Gd^{3+} sublattice to Ce^{4+} centers resulting in hole conductivity via a charge transfer excitation: $Ce^{4+} \rightarrow Ce^{3+}$ + hole.

DOI: 10.1103/PhysRevB.71.045121 PACS number(s): 78.55.−m, 71.55.−i, 72.80.Sk, 32.80.Fb

I. INTRODUCTION

In a large number of laser, phosphor, scintillator and, electroluminescence materials, the excited 5*d* states of lanthanide ions play a crucial role, either as pumping or as emitting states in the luminescence process. The awareness is growing that the energy of these states with respect to the delocalized states of the conduction band (CB) can strongly affect the efficiency of the luminescence process through direct or thermally stimulated ionization of the excited lanthanide ions. Various experimental techniques like absorption, luminescence excitation, x-ray or ultraviolet photoelectron emission, excited-state absorption, or thermoluminescence have been used to determine these energies (see, for example, Refs. 1 and 2). An alternative way to position impurity energy levels relative to the bands of the crystalline host is by means of a photoconductivity study. Pedrini[3,4] and McClure[5] and coworkers systematically studied photoconductivity properties of doped wide band-gap insulators. They positioned ground states of lanthanide ions with respect to the CB bottom by deriving the ionization threshold energies from persistent photoconductivity spectra. Later Raukas[6] *et al.*, Yen,[7] and Happek[8] *et al.* concluded from photoconductivity studies that whenever all 5*d* states are located in the CB no luminescence can be observed. They also observed strong temperature dependence of photocurrents whenever the excited states were located close to but below the CB bottom and related that to thermally activated ionization of the excited impurities. Van der Kolk[9] *et al.* further explored this temperature dependence to accurately position the 5*d* excited states, instead of the 4*f* ground state, of Ce^{3+} in Lu_2SiO_5. In cases where the temperature behavior of the photocurrent was discussed[6–10] only a qualitative relation was suggested with luminescence quenching. Surprisingly, the temperature dependence of photocurrent intensity was never directly compared with the luminescence intensity in a single study. In this work an almost one-to-one relation between luminescence quenching and photoconductivity of $GdAlO_3:Ce^{3+}$ is reported and discussed in terms of a semiquantitative model.

II. EXPERIMENTAL TECHNIQUES

A $5 \times 5 \times 0.3$-mm^3 sized 0.2% Ce^{3+} doped $GdAlO_3$ single crystal was used in the combined photoluminescence (PL) and photoconductivity (PC) study. The apparatus used in the PL and PC study consists of a 150-W Hamamatsu CW Xe lamp coupled to an ARC VM502 vacuum monochromator and a custom built vacuum sample chamber. A Janis VPF-700 liquid-nitrogen cryostat, a Lakeshore 331S temperature controller, a thermocouple, and a cartridge heater allowed for temperature control between 77 and 800 K. Emission spectra were recorded in photon counting mode using a Macam 0.1-m monochromator and a cooled photomultiplier tube. Photocurrents were recorded in a similar way as described earlier[9] with the difference that the nickel mesh electrodes and the sapphire cover plates were replaced by transparent 5-nm-thick Pt/Pd electrodes, sputter deposited using a Cressington argon sputter coater. Some of the optical, luminescence, and scintillator properties of $GdAlO_3$ were described earlier in relation with its potential use as a scintillator.[11–15]

III. RESULTS AND DISCUSSION

A. Room-temperature absorption, photoluminescence, and photocurrent properties

Figure 1 compares the absorption, photoluminescence excitation, and photocurrent excitation spectra recorded at 293 K. The absorption spectrum (dotted line) shows a tail at wavelengths longer than 325 nm. Verweij[14] assigned this absorption feature to Ce^{4+} centers since its strength was found to be related to the Ce^{4+} concentration that could be varied by changing the reducing or oxidizing nature of the synthesis firing atmosphere. Since this tail is also seen in the photocurrent spectrum (dashed line) it can be concluded that the corresponding excitation process leaves mobile charge carriers in the valence band (VB) and therefore most likely correspond to a $VB \rightarrow Ce^{4+}$ charge-transfer (CT) transition.

At higher energy, spectral features of all spectra in Fig. 1 are dominated by the interconfigurational $Ce^{3+}[Xe]4f^1$

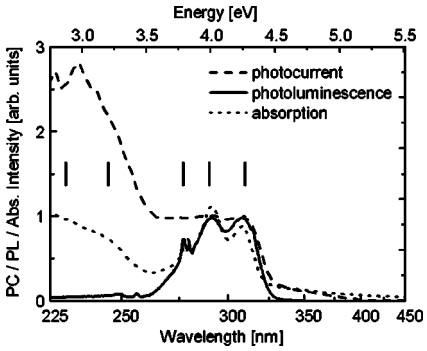

FIG. 1. Absorption spectrum (Abs.), photoluminescence excitation (PL) spectrum, and photocurrent (PC) excitation spectrum of a 0.3-mm-thick $GdAlO_3$:0.2% Ce^{3+} crystal recorded at 293 K. The PL excitation spectrum was obtained using a 0.07% doped crushed crystal.

$\rightarrow$[Xe]$5d^1$ transitions. Their energies as observed in previous studies,[12,14] are indicated in Fig. 1 by vertical lines. Note that the bands at 310, 290, and 277 nm, hereafter referred to as triplet states for convenience, and the bands at 245 and 230 nm (referred to as doublet states) are not fully resolved. The distinction between the triplet and the doublet states can, however, clearly be made. The triplet and the doublet are both observed in absorption (dotted line) with about equal intensity. The PL excitation spectrum, on the other hand (solid line), only reveals the triplet states and shows doublet states of practically zero intensity. The PC excitation spectrum (dashed line) displays the opposite behavior, that is, doublet states of high intensity and triplet states of lower intensity.

A logical explanation of these intensity differences would be that the doublet states are located in the CB, so that optical excitation of these states is followed by autoionization and a corresponding photocurrent. Ionization is not necessarily accompanied by luminescence quenching but can still be followed by radiative recombination at another Ce ion. The low doubled intensity in the PL-excitation spectrum shown in Fig. 1 convincingly demonstrates that in the case of $GdAlO_3$, CB electrons are not retrapped by Ce^{4+} ions to give $5d^1 \rightarrow 4f^1$ emission. Apparently nonradiative recombination has a much higher probability. A sketch of the corresponding level scheme, with the doubled states above and the triplet states below the CB bottom, is shown in Fig. 2(a).

It is interesting to consider an alternative interpretation of the intensity differences discussed above. It is likely that intraconfigurational relaxation within the triplet or within the

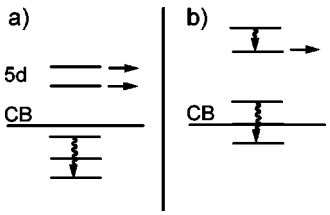

FIG. 2. Sketch of the possible locations of 5*d* energy levels relative to the CB bottom based on absorption, excitation, and photocurrent spectra of $GdAlO_3$:0.2% Ce^{3+} recorded at 293 K.

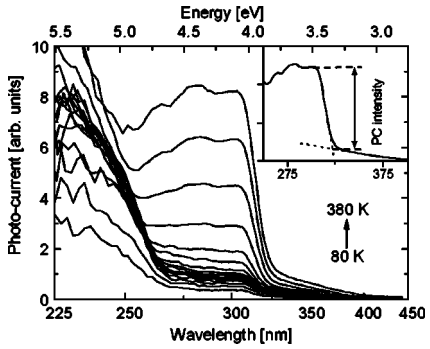

FIG. 3. Photocurrent excitation spectra of a 0.3-mm-thick $GdAlO_3$:0.2% Ce^{3+} crystal between 80 and 380 K in steps of 20 K. The inset demonstrates how it was corrected for the contribution of the CT transition.

doublet is much faster than relaxation from doublet to triplet. Excitation of higher energy triplet levels within the CB [see Fig. 2(b)] may therefore not necessarily result in autoionization but can also result in relaxation to the lowest energy 5*d* state. A comparison between absorption, PL-, and PC-excitation spectra can therefore only give a first estimate of level positions relative to the CB.

Despite the fact that the lowest energy 5*d* state is anticipated below the CB it is, although with reduced intensity, observed in the room-temperature photocurrent spectrum. This points to a thermally stimulated ionization process which will be discussed in the next section.

B. Temperature-dependent photocurrent properties

The temperature dependence of the photocurrent excitation spectrum between 80 and 380 K, presented in Fig. 3, indeed confirms a thermally activated ionization process. The triplet states have low intensity at low temperature but rapidly gain intensity towards higher temperature. At 380 K, triplet intensity has become approximately equal to that of the doublet. A closer inspection of the PC spectra reveals that two temperature regions can be distinguished. At low temperature PC intensity changes only moderately with temperature, while at higher temperature changes are more pronounced. The intensity of the lowest energy 5*d* state as observed in PC spectra was estimated by subtracting the dark conductivity and the contribution of the CT band as indicated by the inset of Fig. 3.

C. Temperature-dependent photoluminescence properties

In order to decide if and to what extent ionization results in luminescence quenching, the temperature dependence of the photoluminescence intensity was calculated from the integral of the emission spectra. Figure 4 displays these emission spectra between 80 and 420 K. The typical $5d \rightarrow 4f$ $Ce^{3+}[^2F_{5/2}, ^2F_{7/2}]$ doublet emission can be observed. The spectral shape is, however, slightly deformed. On the high-energy side the shape of the emission spectra is affected by reabsorption in the crystal. On the low-energy side, non-Ce^{3+}-related emission with a poorly defined spectral shape is

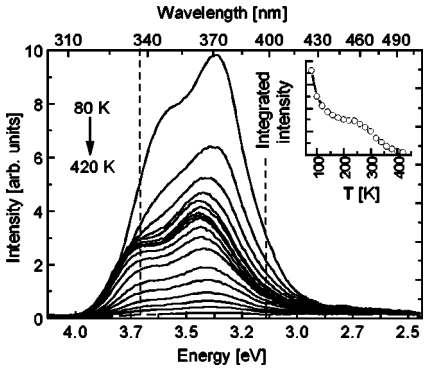

FIG. 4. Emission spectra of a 0.3-mm-thick $GdAlO_3$:0.2% Ce^{3+} crystal between 80 and 420 K in steps of 20 K, upon Ce^{3+} excitation into the lowest energy 5*d* state. The inset displays the integrated luminescence intensity as a function of temperature.

observed. In order to estimate the temperature dependence as accurately as possible, a double Gaussian fit was adopted but only between the dotted vertical lines shown in Fig. 4. The resulting temperature dependence shown in the inset reveals that PL quenching proceeds via two different processes separated by a plateau around 230 K where the PL intensity is relatively insensitive to temperature change.

D. Arrhenius diagram

The temperature dependence of PL and PC, upon excitation into the lowest energy 5*d* state, is summarized in the Arrhenius diagram (Fig. 5) by filled squares and filled circles, respectively. From this figure two things are evident. First, there are two different processes active in $GdAlO_3:Ce^{3+}$ leading to ionization and luminescence quenching. One of them (process I) dominates above 230 K while the other one (process II) is dominant below this temperature. Second, since the slopes of the PC and PL curves are identical but of reversed sign, photoconduction and luminescence quenching must have a common cause. Below, the nature of the two processes will be discussed.

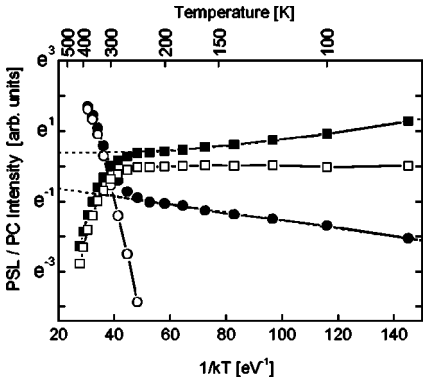

FIG. 5. Temperature dependence of the photocurrent intensity (filled circles) and the integrated Ce^{3+} $5d \rightarrow 4f$ luminescence intensity (filled squares) upon excitation into the lowest energy Ce^{3+} 5*d* state. Dotted lines represent extrapolated fits to the data between 80 and 250 K. The open symbols are obtained after subtraction of the fits from the original data.

Although the temperature dependencies of PL and PC intensity below 230 K can be approximated by a linear fit in the Arrhenius diagram with a slope of 0.01 eV, it is not likely that process II is controlled by a thermally activated process. An activation energy of 0.01 eV is considerably smaller than typical phonon energies of 0.1 eV in ionic lattices. In addition, close inspection of PL data below 230 K reveals a small deviation from perfect Arrhenius behavior which is not expected for a thermally activated process. Instead it is more likely that the temperature dependence of process II originates from $Ce^{3+} \rightarrow Gd^{3+}$ energy transfer. Such transfer is usually followed by energy migration over the Gd^{3+} sublattice to certain quenching centers *X*. This $Ce^{3+} \rightarrow (Gd^{3+})_n \rightarrow X$ type of energy transfer is commonly observed in Gd compounds and is known to be very efficient.[16,17] The first transfer step from Ce^{3+} to Gd^{3+} in $GdAlO_3$ was indeed observed in an earlier scintillation decay study.[13] The second transfer step was studied in a Tb^{3+} co-doped $GdAlO_3:Ce^{3+}$ crystal.[11]

A $Ce^{3+} \rightarrow (Gd^{3+})_n \rightarrow X$ energy transfer can only result in photoconduction, if the final transfer step involves charge transfer. Since it was already established that the CT transition, $VB \rightarrow Ce^{4+}$, resulted in mobile holes, the final transfer step may very well be a Gd^{3+} $^6P \rightarrow {}^8S$ transition in which the transition energy is used to promote an electron from the VB to Ce^{4+} ($VB \rightarrow Ce^{4+}$).

The temperature dependence above 230 K is interpreted as a thermally activated ionization process in which the activation energy barrier ΔE corresponds to the gap between the lowest energy Ce^{3+} 5*d* state and the bottom of the conduction band.[6,9] Since it is our intention to model this thermally activated process (process I) it must be isolated from the influence of process II, therefore experimental data were fitted between 250 and 80 K, extrapolated to higher temperature, and subtracted from the original PL and PC data. Figure 5 shows the extrapolated fits (dotted lines) describing the temperature dependence due to process II only. The resulting data (open symbols), that are obtained after subtraction of the fits from the original data (filled symbols), describe the temperature dependence due to the thermally activated process (process I) and will be used in the model presented below.

E. A model for the temperature dependence of PL and PC

The model anticipated to fit the experimental PL and PC data is schematically summarized in Fig. 6. Optical excitation (c_{12}), radiative recombination (c_{21}), and thermally stimulated ionization (c_{23}) between the Ce^{3+} ground state, the 5*d* excited state, and the conduction band are indicated by straight arrows. (c_{31}) represents the probability of nonradiatively recombination between thermally excited CB electrons and Ce^{4+} ions, either at the originally excited Ce ion or at a different Ce ion. As discussed in Sec. III A, recombination proceeds nonradiatively. This is expected when the formation of a Ce bound exciton (indicated by the dashed line) has a lower energy than the Ce^{3+} 5*d* state.

A quantitative description of the schematic model depicted in Fig. 6 is expressed by the following differential equations (DE's) or rate equations:

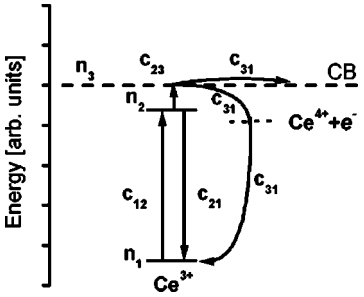

FIG. 6. Schematic representation of the proposed model relating luminescence quenching and photoconduction in Ce^{3+}-doped $GdAlO_3$.

$$n_1' = -c_{12}\cdot n_1 + c_{21}\cdot n_2 + c_{31}\cdot n_3,$$

$$n_2' = c_{12}\cdot n_1 - (c_{21}+c_{23})\cdot n_2,$$

$$n_3' = c_{23}\cdot n_2 - c_{31}\cdot n_3, \tag{1}$$

in which n_1 and n_2 are the fractions of Ce^{3+} ions in the ground state and in the $5d$ excited state, respectively. n_3 equals the number of electrons in the CB and at the same time the number of Ce^{4+} ions, $n' \equiv dn/dt$. The constant coefficients $c_{ij}(s^{-1})$ are given by

$$c_{12} = 10^{-5}, \quad Ce^{3+} \text{ excitation rate},$$

$$c_{21} = 5\times 10^{7}, \quad Ce^{3+} \text{ decay rate } (\tau = 20 \text{ ns}),$$

$$c_{23} = f_0\cdot e^{-\Delta E/k\cdot T}, \quad \text{thermally stimulated ionization rate},$$

$$c_{31} = 10^{10}, \quad \text{electron–}Ce^{4+} \text{ recombination rate } (\tau = 0.1 \text{ ns}). \tag{2}$$

f_0, ΔE, and k are the attempt frequency, the energy difference between the lowest energy $Ce^{3+}5d$ state, and the CB and Bolzmann's constant respectively. c_{12} is equal to the product of the photon flux ($\approx 10^{12}$ s^{-1} cm^{-2}) and the absorption cross section ($\approx 10^{-16}$ cm^2) and the illuminated surface area. c_{31} is determined by the lifetime of the electrons in the CB that can only be estimated. Note that c_{31} and c_{12} strongly affect the magnitude of the PL and PC intensity. They do not, however, affect the temperature dependence and possible errors in their values therefore have no consequences for the discussion below.

For a given set of numerical values of the constant coefficients, the three coupled DE's can be solved numerically for $n_i(t)$, using initial values $n_1(0)=1$, $n_2(0)=0$, and $n_3(0)=0$, to obtain steady-state values (taking t sufficiently large) for n_1, n_2, and n_3. The temperature dependence of the photocurrent and photoluminescence are finally calculated by using the relations

$$PC \propto n_3, \quad \text{photocurrent (arb. units)},$$

$$PL \propto c_{21}\cdot n_2, \quad \text{photoluminescence (arb. units)}, \tag{3}$$

and solving the DE's repeatedly for all temperature values of interest.

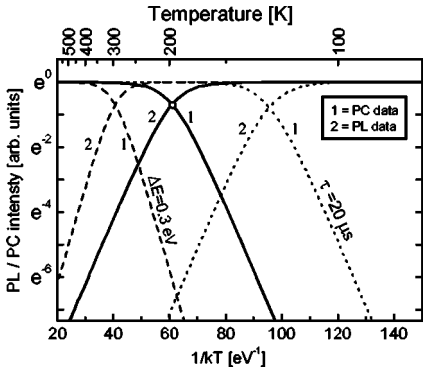

FIG. 7. Calculated temperature dependence of the photocurrent intensity and the luminescence intensity upon Ce^{3+} excitation between 80 and 600 K. Solid lines: $f_o=10^{13}$ Hz, $\Delta E=0.2$ eV, and $\tau=20$ ns. Dashed lines: $f_o=10^{13}$ Hz, $\Delta E=0.3$ eV, and $\tau=20$ ns. Dotted lines: $f_o=10^{13}$, $\Delta E=0.2$ eV, and $\tau=20$ μs.

Results of such calculations between 80 and 600 K are given in Fig. 7. It shows the general temperature behavior of PL and PC intensity upon excitation into the lowest energy $5d$ state of Ce^{3+}. The solid lines are calculations using typical values: $f_o=10^{13}$ Hz, $\Delta E=0.2$ eV, and $\tau=20$ ns. At low temperature PL has maximum intensity (limited by the excitation rate) since loss of intensity due to ionization is practically absent. At high temperature the situation is reversed and PC has maximum intensity since the ionization rate is orders of magnitude higher than the radiative decay rate. Only an experiment operating in the temperature region near the crossover point (the point where PC and PL have equal intensity) indicated by the open circle, will display a clear anticorrelation between PL and PC intensity. Outside this region either PL or PC has a detectable change with temperature and one may be inclined to conclude that PL and PC intensity are unrelated. Note how the crossover point is affected when the decay time is changed to a value of 20 μs more typical for $4f \rightarrow 4f$ transition (dotted lines) instead of 20 ns. It is therefore not unlikely that luminescence quenching from certain $4f$ levels (like the $^5D_4$ level of Tb^{3+} in ZrO_2) due to ionization can be observed as well. When ΔE is changed to 0.3 eV (see dashed lines) not only the crossover point but also, as expected, the slopes are affected. Figure 7 not only related PC intensities with PL intensities, it also makes clear that ionization energy barriers and thus the position of impurity energy levels can be determined with an accuracy significantly smaller than 0.1 eV. Figure 7 also directly gives the quantum efficiency (QE) of ionization. For example, the solid line in Fig. 7 gives a 50% QE for thermal ionization at about 200 K and a QE close to 100% at room temperature. Using the $5d$ intensity ratios as observed in PC excitation spectra, the QE for autoionization from $5d$ states located in the CB can be found as well.

In Fig. 8 the model is fitted to the experimental data taken from Fig. 5 (open symbols). The best fit (solid line) to the PC experimental data (squares) was obtained using $f_0=1.5\times 10^{12}$ Hz and $\Delta E=0.34$ eV. It can therefore be concluded that the lowest energy $5d$ state of Ce^{3+} is positioned 0.34 eV below the CB bottom. For these values,

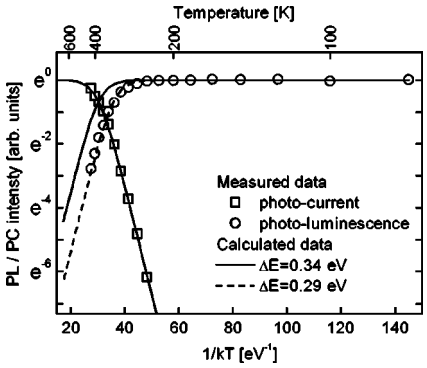

FIG. 8. Calculated (solid and dashed lines) and measured (symbols) temperature dependence of the photocurrent intensity (squares) and the integrated Ce^{3+} $5d \rightarrow 4f$ luminescence intensity (circles).

however, a noticeable mismatch between the measured (circles) and calculated PL data (solid line) becomes apparent. To simultaneously fit both PL and PC data it is necessary to allow for different activation energies for luminescence quenching and photocurrent generation. When a smaller activation energy of 0.29 eV for PL quenching is chosen a good fit to the PL data is obtained (dashed line). A slightly smaller activation energy for luminescence quenching than for photocurrent generation suggests that luminescence quenching takes place predominantly at the excited Ce^{3+} ion. In that case the formation of a bound exciton does not involve the complete removal of an electron from Ce^{3+} and will therefore cost less energy. In the case of ionization the electron has to overcome the Coulomb attraction of Ce^{4+} which requires more energy.

We finally wish to note that the model presented assumes that the electron-Ce^{4+} recombination rate, equal to $c_{31} \cdot n_3$, is independent of the Ce^{4+} concentration. This is in contradiction to the nature of the photoconductivity that is assumed, i.e., a $Ce^{3+} \rightarrow Ce^{4+}$ CT transition. One must not forget, however, that the number of Ce^{4+} ions that are intrinsically present in the crystal (N_3) exceeds the number of Ce^{4+} ions ()that are optically generated (n_3) by several orders of magnitude. The change in the total number of Ce^{4+} (n_3+N_3) ions can therefore be neclected in good approximation. Indeed, when $c_{31} \cdot n_3$ is replaced by $c'_{31} \cdot n_3 \cdot (n_3+N_3)$ in the rate equations the same PC temperature dependence is calculated. Note that n_3 is equal to the number of optically generated Ce^{4+} ions and, within this model, also to the number of CB electrons.

IV. CONCLUSIONS

Luminescence quenching of Ce^{3+} in $GdAlO_3$ is due to two different processes involving ionization. One dominates below 230 K and corresponds to a $Ce^{3+} \rightarrow (Gd^{3+})_n \rightarrow X$ energy transfer. X are quenching centers that, at least partly, consist of Ce^{4+} ions. The other quenching process dominates above 230 K and corresponds to thermally activated ionization of excited Ce^{3+} centers. A fit by a model describing the temperature dependence of the PL and PC intensity reveals (i) that the emitting $5d$ state of Ce^{3+} is positioned 0.34 eV below the CB bottom, (ii) a 0.05-eV smaller activation energy for PL quenching than for PC generation, and (iii) that luminescence quenching predominantly proceeds at the Ce^{3+} ion that was excited.

ACKNOWLEDGMENT

This work was supported by the Dutch Technology Foundation (STW).

[1] S. A. Basun, T. Danger, U. Happek, A. A. Kaplyanskii, D. S. McClure, K. Petermann, and W. C. Wong, Phys. Rev. B **54**, 6141 (1996).
[2] C. Dujardin, C. Pedrini, J. C. Gacon, A. G. Petrosyan, A. N. Belsky, and A. N. Vasilev, J. Phys.: Condens. Matter **9**, 5229 (1997).
[3] C. Pedrini, D. S. McClure, and C. H. Anderson, J. Chem. Phys. **70**, 4959 (1979).
[4] C. Pedrini and F. Rogemond, J. Appl. Phys. **59**, 1196 (1986).
[5] D. S. McClure and C. Pedrini, Phys. Rev. B **32**, 8465 (1985).
[6] M. Raukas, S. A. Basun, W. van Schaik, W. M. Yen, and U. Happek, Appl. Phys. Lett. **69**, 3300 (1996).
[7] W. M. Yen, J. Lumin. **83-84**, 399 (1999).
[8] U. Happek, S. A. Basun, J. Choi, J. K. Krebs, and M. Raukas, J. Alloys Compd. **303-304**, 198 (2000).
[9] E. van der Kolk, S. A. Basun, G. F. Imbusch, and W. M. Yen, Appl. Phys. Lett. **83**, 1740 (2003).
[10] S. A. Basun, M. Raukas, U. Happek, A. A. Kaplyanskii, J. C. Vial, J. Rennie, W. M. Yen, and R. S. Meltzer, Phys. Rev. B **56**, 12 992 (1997).
[11] J. Fava, G. LeFlem, J. C. Bourcet, and F. Gaume-Mahn, Mater. Res. Bull. **11**, 1 (1976).
[12] J. A. Mares, C. Pedrini, B. Moine, K. Blazek, and J. Kvapil, Chem. Phys. Lett. **206**, 9 (1993).
[13] J. A. Mares, M. Nikl, C. Pedrini, D. Bouttet, C. Dujardin, B. Moine, J. W. M. Verweij, and J. Kvapil, Radiat. Eff. Defects Solids **135**, 369 (1995).
[14] J. W. M. Verweij, M. Th. Cohen-Adad, D. Bouttet, H. Lautesse, B. Moine, and C. Pedrini, Chem. Phys. Lett. **239**, 51 (1995).
[15] P. Dorenbos, E. Bougrine, J. T. M. de Haas, C. W. E. van Eijk, and M. V. Korzhik, Radiat. Eff. Defects Solids **135**, 321 (1995).
[16] G. Blasse, Recl. Trav. Chim. Pays-Bas **105**, 143 (1986).
[17] P. Dorenbos, J. C. van 't Spijker, and C. W. E. van Eijk, *Proceedings of the International Conference on Inorganic Scintillators and Their Applications, Shanghai, 1997*, edited by Y. Zhiwen, F. Xiqi, L. Peijun, and X. Zhilin (Shanghai Branch Press, Shanghai, 1997).